Journal of Biomolecular NMR, 9 (1997) 259–272
ESCOM

J-Bio NMR 427

Assignment methodology for larger RNA oligonucleotides: Application to an ATP-binding RNA aptamer

Thorsten Dieckmann and Juli Feigon*

Department of Chemistry and Biochemistry and Molecular Biology Institute, University of California, P.O. Box 951569, Los Angeles, CA 90095-1569, U.S.A.

Received 18 October 1996
Accepted 17 December 1996

Keywords: In vitro selection; AMP; Heteronuclear NMR; Specific labeling; RNA structure

Summary

The use of uniform $^{13}C,^{15}N$ labeling in the NMR spectroscopic study of RNA structures has greatly facilitated the assignment process in small RNA oligonucleotides. For ribose spin system assignments, exploitation of these labels has followed previously developed methods for the study of proteins. However, for sequential assignment of the exchangeable and nonexchangeable protons of the nucleotides, it has been necessary to develop a variety of new NMR experiments. Even these are of limited utility in the unambiguous assignment of larger RNAs due to the short carbon relaxation times and extensive spectral overlap for all nuclei. These problems can largely be overcome by the additional use of base-type selectively $^{13}C,^{15}N$-labeled RNA in combination with a judicious use of related RNAs with base substitutions. We report the application of this approach to a 36-nucleotide ATP-binding RNA aptamer in complex with AMP. Complete sequential ^{1}H assignments, as well as the majority of ^{13}C and ^{15}N assignments, were obtained.

Introduction

The structure determination of nucleic acids by NMR spectroscopy depends on an unambiguous assignment of as many proton resonances as possible, and for larger RNAs carbon and nitrogen resonances as well. The assignment of RNA is considerably more difficult than for DNA of similar size. This is mainly due to the much narrower spectral dispersion of the 2', 3', 4', and 5' ribose protons relative to DNA. In addition, the preferred conformation of the ribose in RNA (C3'-endo) has very small H1'-H2' couplings, and this severely limits the sensitivity of any experiment using these couplings. Finally, the 'historic' methodology for sequential assignment of nucleic acids via homonuclear NMR techniques (Feigon et al., 1983; Hare et al., 1983; Scheek et al., 1983) relies on the assumption of a helical structure and therefore fails in the case of RNAs with unknown, nonhelical structures. Thus, until recently only the structures of fairly small RNA molecules with mostly regular structure have been determined by NMR (Varani and Tinoco, 1991; Moore, 1993).

A major breakthrough for the assignment of RNA was the introduction of methods for the labeling of RNA with ^{13}C and ^{15}N (Batey et al., 1992; Nikonowicz et al., 1992) and the development of heteronuclear NMR techniques analogous to those used in protein NMR spectroscopy (Dieckmann and Feigon, 1994; Pardi, 1995; Varani et al., 1996). This has greatly improved the structure determination of even small RNA oligonucleotides, since many more resonances can now be assigned. However, in the case of RNAs with more than 30 nucleotides, uniform $^{13}C,^{15}N$ labeling of samples still does not completely solve the assignment problem. The first major difficulty is to resolve ambiguities which are due to the extreme overlap of the ribose resonances. Even carbon-resolved NOESY experiments (Marion et al., 1989; Zuiderweg et al., 1990, 1991) can often only provide partial assignments because of the highly degenerate chemical shifts in both the carbon and proton dimensions. Another major difficulty is differentiating sequential from long-range NOEs. In the absence of reliable methods for the direct through-bond assignment of neighboring nucleotides, it is easy to make mistakes in assignments. This problem illustrates the

*To whom correspondence should be addressed.

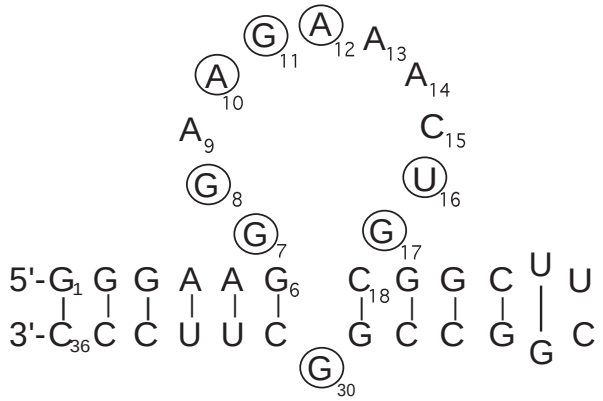

Fig. 1. Sequence and secondary structure of the ATP-binding RNA aptamer used in this study. The consensus sequence from Sassanfar and Szostak (1993) comprises only the internal loop and the single bulged G. Nucleotides that are highly conserved are circled.

major difference in comparison to proteins, where direct sequential assignments can be obtained even for fairly large systems (ca. 280 residues, comparable in molecular mass to 93 RNA nucleotides) (Clore and Gronenborn, 1993; Cavanagh et al., 1996). The assignments for large RNAs with nonhelical structures cannot at the present time be achieved purely by NMR methods, but require the extensive use of selective labeling and base substitutions (Michnicka et al., 1993; Battiste et al., 1995; Varani et al., 1996).

We have developed an efficient strategy for the assignment and structure determination of larger RNA molecules and especially RNA–ligand systems, which will be demonstrated on the example of the ATP-binding RNA aptamer (Sassanfar and Szostak, 1993). The structure of this RNA in complex with its ligand AMP/ATP has recently been solved independently by two laboratories (Dieckmann et al., 1996; Jiang et al., 1996), using quite different approaches to solve the problems resulting from the relatively large size of the molecule and the unknown and nonpredictable structure of the binding region. The aptamer was discovered by in vitro selection (Ellington and Szostak, 1990; Tuerk and Gold, 1990). The consensus sequence contains an 11 base loop opposite a single bulged G and flanked by two stem regions (Fig. 1) (Sassanfar and Szostak, 1993). The sequence of the stems has only very little influence on binding, but the internal loop is highly structured and contains mostly conserved bases. The aptamer is one of the largest RNA molecules for which a structure has been determined by NMR spectroscopy (Feigon et al., 1996; Varani et al., 1996). The major problems in obtaining unambiguous resonance assignments were the severe resonance overlap for protons and heteronuclei and the unknown and nonhelical structure of the binding pocket. To resolve these problems we used a combination of various NMR techniques and base-type specific labeling of the RNA as well as RNAs with base substitutions.

Materials and Methods

Sample preparation

The RNA was synthesized enzymatically on a DNA template using T7 RNA polymerase and unlabeled NTPs (Milligan et al., 1987) and/or ^{13}C,^{15}N-labeled NTPs to prepare unlabeled, base specifically G-, A-, or U/C-labeled, or fully labeled RNA samples. The labeled NMPs were isolated from methanolotrophic bacteria which had been grown on ^{13}C-methanol and ^{15}N-ammonia, purified, and converted to NTPs as described (Batey et al., 1992; Peterson et al., 1994). For selectively labeled samples, the mixture of NTPs was separated into the four nucleotides by HPLC using a semipreparative scale C_{18} column (Wa-

TABLE 1
SUMMARY OF HETERONUCLEAR NMR EXPERIMENTS

Experiment	Sample with label on			Time domain size (points) F1 × F2 (× F3)	Sweep widths (Hz) F1 × F2 (× F3)	Carrier frequency (ppm)	Total time (h)
	RNA	AMP	A, G or C,U only				
2D ^{1}H-^{13}C ct HSQC	X	X	X	256 × 1024	7550 × 5000	80, 4.7	14
2D ^{1}H-^{15}N HMQC	X	X	X	128 × 1024	4054 × 10000	110, 4.7	12
2D HCN	X		X	128 × 1024	1946 × 6010	157, 4.7	4
2D HCNCH			X	48 × 1024	840 × 4195	157, 5.5	12
2D HCCNH-TOCSY			X	64 × 2048	780 × 13227	147, 4.7	24
2D ^{1}H-^{15}N long-range HSQC	X	X	X	256 × 1024	3012 × 7246	190, 7.7	18
2D AH2 HCCH-TOCSY	X		X	256 × 1024	5000 × 5000	145, 4.7	18
3D HCCH-TOCSY/COSY			X	160 × 128 × 512	1500 × 4400 × 4032	77.5, 4.7	72
2D NOESY with ^{13}C-filter			X	512 × 2048	5000 × 5000	110, 4.7	24
2D ^{1}H-^{13}C HMQC-NOESY		X	X	128 × 2048	7550 × 5000	110, 4.7	18
2D ^{1}H-^{13}C HSQC-NOESY WG		X	X	128 × 2048	7500 × 10000	110, 4.7	18
2D ^{1}H-^{15}N HSQC-NOESY WG		X	X	128 × 2048	4560 × 10000	120, 4.7	24
3D ^{1}H-^{13}C NOESY-HMQC	X		X	160 × 96 × 512	5000 × 4400 × 5000	77.5, 4.7	72
3D ^{1}H-^{15}N NOESY-HMQC	X		X	160 × 92 × 512	5000 × 7500 × 5000	120, 4.7	72

ters: PrepPak Cartridge, 25×100 mm) with a water/methanol gradient. Three base-type specifically labeled samples were prepared using labeled A, G, or C/U nucleotides and commercial, nonlabeled nucleotides for the rest. After enzymatic synthesis, the RNA was purified and NMR samples were prepared as previously described (Peterson et al., 1994; Dieckmann et al., 1996). Samples of the wild-type RNA aptamer used in obtaining assignments included (i) unlabeled RNA with unlabeled AMP; (ii) unlabeled RNA with labeled AMP; (iii) unlabeled RNA with unlabeled ATP; (iv) labeled RNA with unlabeled AMP; (v) G-labeled RNA with unlabeled AMP; (vi) A-labeled RNA with unlabeled AMP; and (vii) C,U-labeled RNA with unlabeled AMP in both H_2O and D_2O. In addition, samples of RNAs with base substitutions (G7A, G8A, A9U, C15U, G17A, C18U/G29A) were used to confirm the assignments. An additional RNA sample was prepared synthetically on an ABI392 DNA synthesizer using β-cyanoethyl RNA phosphoramidites except for an ABI fast phosphoramidite deoxy G at nucleotide 11. NMR samples of the aptamers were typically 0.5–1.6 mM in RNA, pH 6.0, 100 mM NaCl.

NMR spectroscopy

All heteronuclear NMR spectra were acquired at 500 MHz on Bruker AMX and DRX spectrometers. Homonuclear spectra were acquired at 500 and 750 MHz on Bruker DRX and DMX spectrometers. The heteronuclear experiments used are summarized in Table 1. Acquisition and processing parameters for specific experiments are given in the figure legends. Processing and spectral analysis were performed using the program packages XWIN-NMR 1.2 and AURELIA 2.0 (Bruker Inc., Rheinstetten, Germany).

Results and Discussion

Overall strategy

The overall assignment strategy involved the iterative analysis of NMR spectra acquired on unlabeled, partially

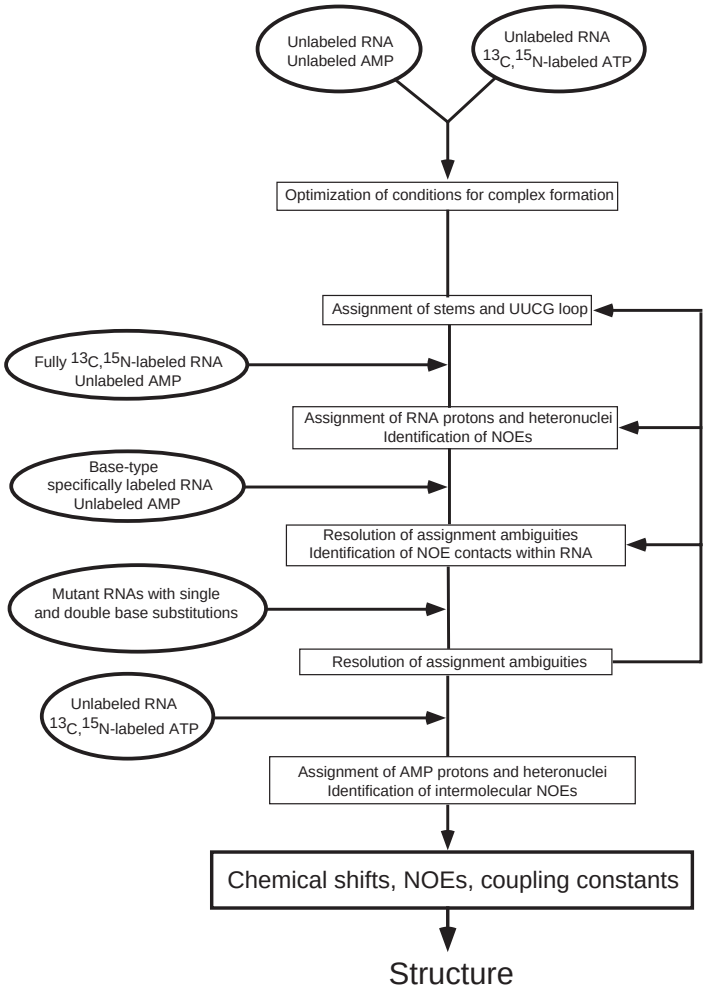

Fig. 2. Schematic of the overall strategy for the assignment and structure determination of the ATP-binding RNA aptamer. The ovals represent the different samples used in the assignment process and the boxes give the major steps in the process as well as the type of extracted information. The arrows at the right indicate the iterative application of the assignment steps.

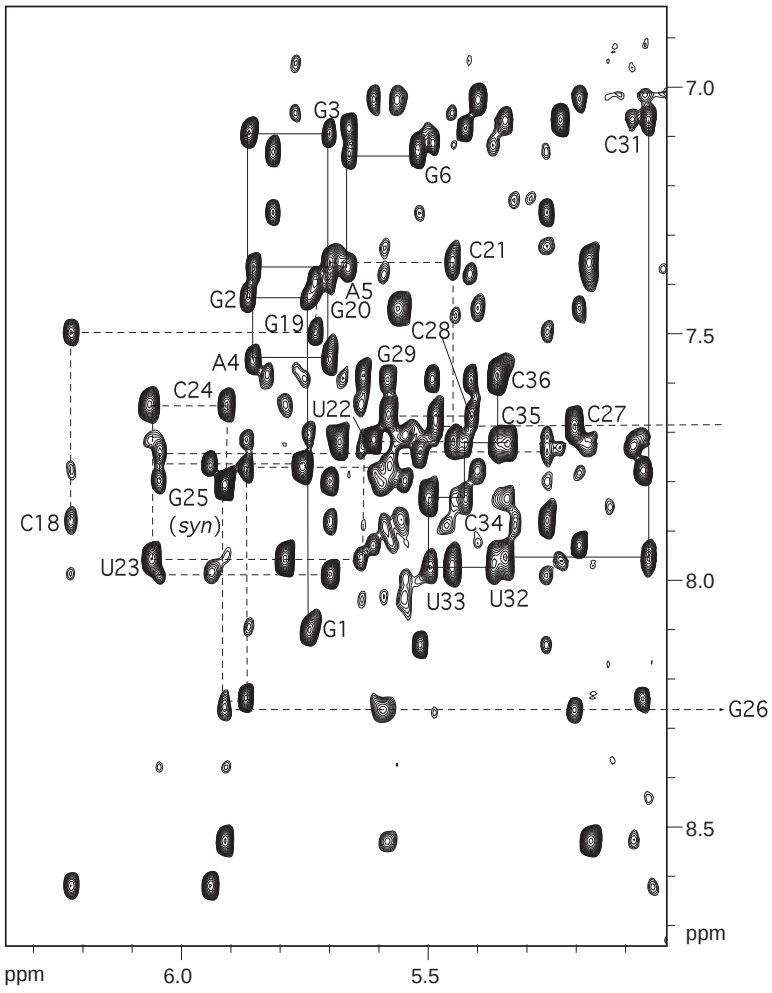

Fig. 3. H1' to base proton region of a 750 MHz NOESY spectrum (mixing time 300 ms) of a 1:1 AMP:RNA complex (unlabeled) at 283 K. The sequential assignments for the stems and the UUCG tetraloop are traced with solid lines for the left stem and dashed lines for the right stem, and the H1' to base intranucleotide cross peaks are labeled. In t_2 and t_1, 1024 and 300 complex points were acquired, respectively, with 64 scans per t_1 increment and States-TPPI phase cycling. The final data matrix was 2048×2048 points and was processed with a Gaussian filter function (LB −18, GB 0.08 in F2 and 0.14 in F1).

labeled, and fully ^{13}C,^{15}N-labeled wild-type aptamer RNA complexed with labeled or unlabeled AMP, as well as RNA samples with base substitutions (Fig. 2). As a starting point, unlabeled samples of the aptamer were titrated with AMP or ATP to monitor the binding of the ligand as a function of pH, salt concentration, and ligand concentration. Once the optimal conditions for binding were found, a sample with ^{13}C,^{15}N-labeled AMP was used to check for complex formation by observing the ligand directly. Initial assignments for the regions with regular secondary structure, the stems and the UUCG tetraloop, were obtained by standard methods based on homonuclear 2D NMR techniques (Wüthrich, 1986; Feigon et al., 1992). Additional assignments were then obtained from fully ^{13}C,^{15}N-labeled RNA in complex with unlabeled AMP, although the tremendous overlap, both in carbon and proton spectra, did not allow a complete assignment using the fully labeled sample alone. The fast T_2 relaxation of protons and especially ribose carbons limited the utility of experiments employing PC transfers for correlation via the phosphodiester backbone (Heus et al., 1994; Marino et al., 1994b,1995), NMR techniques which could in principle provide direct, unambiguous assignments via the nucleic acid backbone. Therefore, the majority of the assignments were obtained on base-type specifically labeled ATP-binding aptamer samples complexed with unlabeled AMP. These samples with ^{13}C,^{15}N labels on G, A, or C/U provided increased resolution and unambiguous assignment of the resonances to base type. In addition, they made it possible to distinguish between many intra- and interresidue NOEs in a straightforward way by the application of carbon- and nitrogen-filtered/selected experiments. Once most of the RNA signals were assigned, unlabeled samples of aptamers with single base mutations were used to identify problems in the assignments and provide additional evidence for ambiguous assignments. Assignment of the AMP proton and heteronuclear NMR spectra as well as the identification of aptamer–ligand

NOEs was achieved on samples with $^{13}C,^{15}N$-labeled AMP and unlabeled RNA, which allowed the selective observation of the signals originating from bound ligand without the interference of RNA signals.

Identification of optimal solution conditions

The best conditions for the investigation of the aptamer complex by NMR were determined by titration of low-concentration (~0.1 mM) RNA samples with unlabeled AMP at salt concentrations between 0 and 300 mM NaCl, pH values between 4.5 and 6.5, and in the presence and absence of 1–5 mM $MgCl_2$. Optimal spectra were obtained at pH 6.0 in 100 mM NaCl and without magnesium with an RNA:AMP ratio of 1:1 or up to ca. 10% excess AMP. One-dimensional NMR spectra with $1\bar{1}$-echo water suppression (Sklenář and Bax, 1987) were used to follow the progress of the titrations by monitoring changes in the imino region of the spectrum. Several isolated RNA imino resonances can be observed for the complexed and the free form of the aptamer, and their intensity changes over the course of the titration allowed an estimation of the amount of free and bound RNA. The amount and specificity of binding at the optimal conditions were assayed by ^{1}H-^{13}C correlation (Piantini et al., 1982) spectra measured on a complex formed between $^{13}C,^{15}N$-labeled AMP and unlabeled RNA. Only very little or no free AMP can be detected in these spectra as long as there is uncomplexed aptamer present. Only one set of signals for the bound and one set of signals for the free AMP were observed under all conditions tested, independent of the RNA and AMP concentration.

Unlabeled RNA and AMP: Assignment of stem regions and UUCG tetraloop

Well-established methods exist for the assignment of DNA or RNA NMR spectra as long as the molecules have a more or less regular helical structure (Wüthrich, 1986; Feigon et al., 1992). In the case of the ATP-binding RNA aptamer, the stems of the RNA could readily be assigned from the unlabeled sample alone using NOESY spectra in 90% H_2O and 100% D_2O. These assignments were facilitated by the characteristic GGG sequence at the 5' end and the UUCG tetraloop, which had previously been well characterized by NMR (Cheong et al., 1990; Allain and Varani, 1995). The base and anomeric protons of nucleotides 1–6, 18–29, and 31–36 were assigned using the standard sequential H1'-H8/H6 connectivities (Fig. 3). In addition, all imino protons in the two stems (except G1, which does not appear in the spectra due to fast exchange with H_2O) were assigned via sequential imino–imino connectivities present in 2D NOESY spectra of the sample in H_2O (Fig. 4). However, assignments for the exchangeable and nonexchangeable resonances of the remaining nucleotides (internal loop) could not be made with any certainty from the homonuclear data since sequential and nonsequential NOE connectivities could not be a priori distinguished in the absence of knowledge of the loop fold. For some residues, either no or several possible sequential connectivities were observed.

Fully $^{13}C,^{15}N$-labeled RNA in D_2O: Initial assignments of internal loop residues

The next step in the assignment procedure was to obtain heteronuclear NMR spectra on a uniformly $^{13}C,^{15}N$-labeled RNA sample complexed with unlabeled ligand. Use of the unlabeled ligand allowed the observation of the RNA aptamer signals without interference of the ligand resonances. Most of the NMR experiments used can be classified into two categories: (i) methods for the correlation of signals within or between neighboring

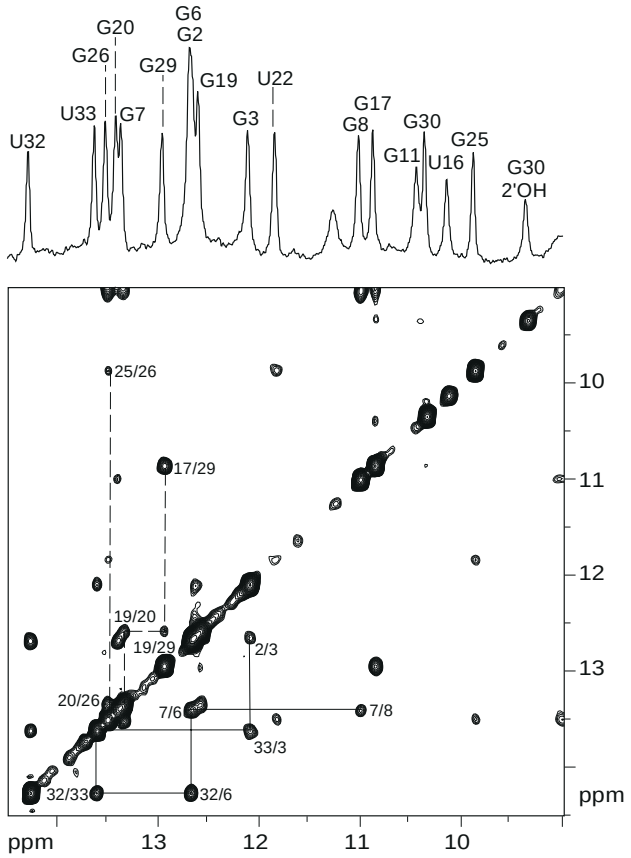

Fig. 4. One-dimensional spectrum in H_2O (imino region only) and corresponding part of a 2D NOESY of the unlabeled aptamer with unlabeled AMP. The assignments of the two stem regions and the UUCG loop are marked with solid lines for the left stem and dashed lines for the right stem. Both spectra were acquired at 278 K with $1\bar{1}$-echo water suppression (excitation maximum at 12.0 ppm) on a sample containing 1.4 mM of 1:1 RNA:AMP complex. The 1D spectrum was measured with 8K complex points and transformed after multiplication with an exponential function (line broadening 15 Hz) to a size of 8K. The 2D spectrum was acquired using 64 scans with 1024 and 150 complex points in F2 and F1, respectively. States-TPPI phase cycling was applied in F1. The final data matrix was 2048 $\times$ 1024 points and was processed with a Gaussian filter function (LB –25, GB 0.1 in F2 and 0.18 in F1).

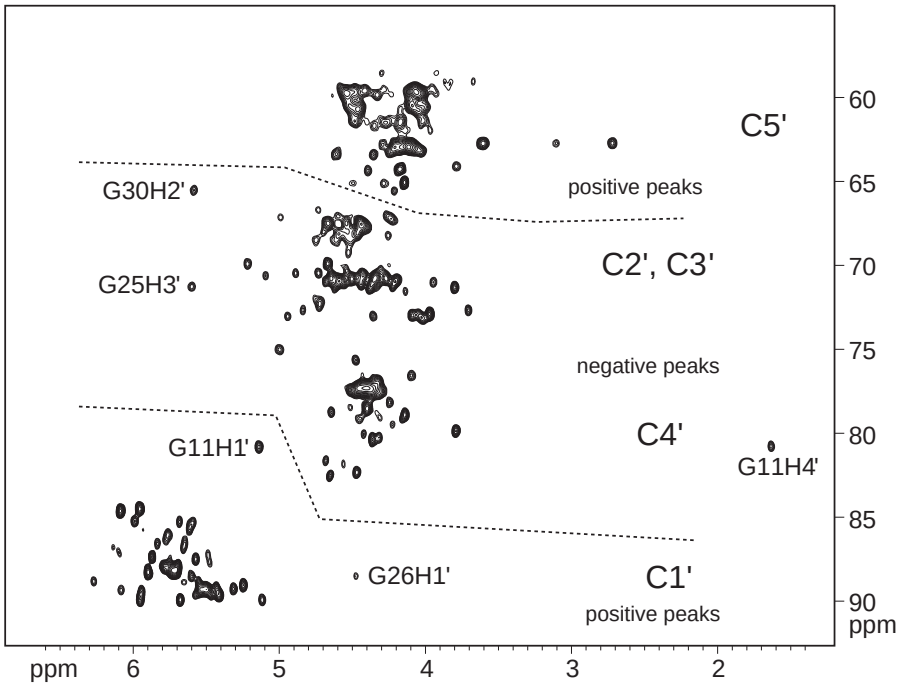

Fig. 5. ^{1}H-^{13}C constant-time HSQC spectrum of the fully ^{13}C,^{15}N-labeled aptamer in complex with unlabeled AMP. The constant-time evolution delay for carbon was set to $1/J_{CC}$, resulting in opposite phases for the C1', C5' and C2', C3', C4' cross peaks. Some of the strongly shifted resonances are labeled. The spectrum was acquired at 293 K in D_2O with low-power saturation of the residual HDO resonance on a sample containing 1.1 mM of RNA in complex with an equimolar amount of AMP in 100 mM NaCl at pH 6.0. 1024 and 64 complex points in F2 and F1, respectively, with 64 scans per t_1 increment were acquired. States-TPPI phase cycling was applied in F1. The final data matrix was 2048×1024 points and was processed with a Gaussian filter function (LB –25, GB 0.1) in F2 and a 90° shifted squared sine bell in F1.

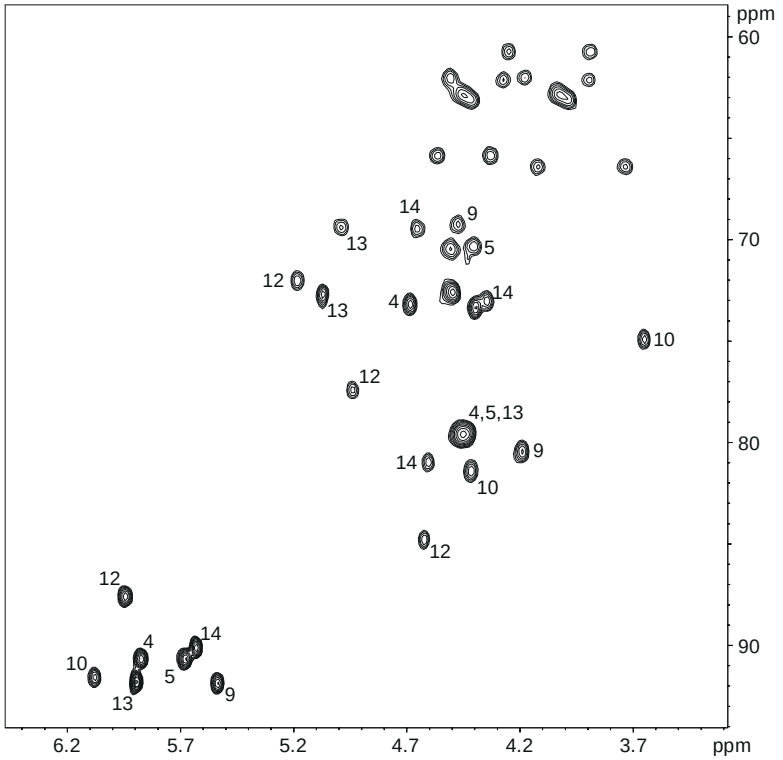

Fig. 6. ^{1}H-^{13}C constant-time HSQC spectrum of the A-labeled aptamer in complex with unlabeled AMP at 293 K in D_2O measured with low-power saturation of the residual HDO resonance (0.9 mM of 1:1 RNA:AMP). The 1', 2', 3' and 4' cross peaks are labeled. 1024 and 64 complex points in F2 and F1, respectively, with 128 scans per t_1 increment were acquired. States-TPPI phase cycling was applied in F1. The final data matrix was 2048×1024 points and was processed with a Gaussian filter function (LB –25, GB 0.1) in F2 and a 90° shifted squared sine bell in F1.

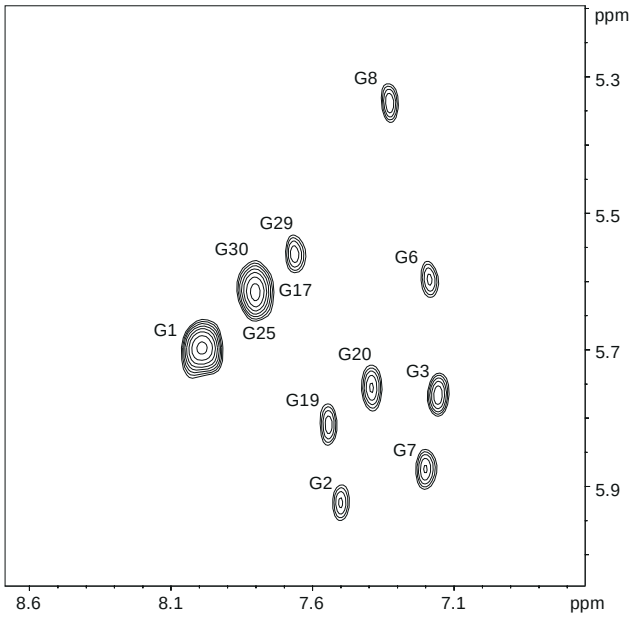

Fig. 7. Two-dimensional HCNCH spectrum of G-labeled RNA ATP binder in complex with unlabeled AMP (measured at 293 K, 1.0 mM 1:1 RNA:AMP complex). Nine out of the 12 signals present are resolved. Two resonances (G11 and G26) are missing in the spectrum due to the unusual chemical shifts of their H1'/C1' resonances, which are located outside the excitation range of the selective pulses used in the experiment. The spectrum was acquired with 1024 and 48 complex points in t_2 and t_1, respectively, 1024 scans per t_1 increment, was apodized with a 60° and 75° shifted squared sine bell in t_2 and t_1, and was zero filled to 1024 points in both dimensions.

nucleotides; and (ii) methods that reduce the overlap in homonuclear spectra, especially NOESY experiments, by labeling the signals according to the frequencies of their associated heteronuclei.

Initial classification of the nonexchangeable proton resonances by type was done from ^{1}H-^{13}C (Santoro and King, 1992; Vuister and Bax, 1992) and long-range ^{1}H-^{15}N correlation (Sklenář et al., 1994) spectra of the HMQC or HSQC type, based on the characteristic chemical shifts or coupling patterns of their correlated heteronuclei. The UH5, CH5, UH6/CH6, GH8/AH8, and AH2 are resolved in both the nitrogen and carbon experiments. Identification of the AH2 is especially important for the interpretation of NOESY spectra, since it is difficult to distinguish the AH2 from other aromatic resonances in any other way. The identified AH2 were connected to their corresponding H8/C8 in an HCCH-TOCSY experiment (Legault et al., 1994; Marino et al., 1994a). The ^{13}C experiments resolve most of the H5'/H5", H4', H1', and H2'/H3' into distinct spectral regions. Ambiguities were resolved using the constant-time version of the ^{1}H-^{13}C HSQC (Santoro and King, 1992) experiment with the constant-time delay set to $1/J_{CC}$ (Battiste et al., 1995), which identifies nucleotides with unusual chemical shifts in the ^{13}C dimension. Since the relative phase of the cross peaks depends on the number of coupled carbons, the C1' and C5' cross peaks have a phase opposite to signals originating from the rest of the ribose carbons (Fig. 5). The ATP-binding aptamer shows a number of strongly shifted resonances; the most remarkable ones are the H4' of G11 at 1.68 ppm, the C1' of G11 at 80.8 ppm, and the H2' of G30 at 5.59 ppm (Fig. 5). Without the constant-time HSQC, the C1' of G11 could easily have been mistaken for a 4' carbon.

Once the base type and H1' resonances were identified, the next problem was to distinguish intranucleotide from internucleotide base-H1' cross peaks as a first step in sequential assignment. With a labeled sample this problem can in principle be solved by a direct through-bond correlation of the H1' and H8/H6 protons via the carbons and nitrogens. However, there are several problems connected with this approach. Even though there are a large number of NMR techniques available to achieve this kind of correlation (Dieckmann and Feigon, 1994; Pardi, 1995), they all follow only two different strategies. Either they connect the anomeric and base protons in one experiment using the heteronuclear one- or two-bond couplings with the intermediate carbons and nitrogens (HCNCH experiments) (Farmer et al., 1993; Sklenář et al., 1993b; Tate et al., 1994) or they correlate both protons to the same heteronucleus using separate experiments (HCN experiments) (Sklenář et al., 1993a; Müller et al., 1994). The HCNCH experiments give spectra which are easy to interpret and have the least overlap problems, but they require very long transfer times. Thus, the sensitivity of these experiments is limited by the short carbon T_2 of larger RNAs. The two-experiment (HCN) approach is of higher sensitivity, but is limited by the poor resolution of the nuclei used to connect the two spectra (usually N9/N1). In the case of the fully ^{13}C,^{15}N-labeled ATP-binding aptamer, only ca. 30% of the H1' to H8/H6 cross peaks could be unambiguously assigned using 2D HCN experiments (Sklenář et al., 1993a). A 2D HCNCH experiment (Sklenář et al., 1993b) gave better results, although even here the fully labeled sample did not allow the identification of all intranucleotide connectivities. The combination of both methods provided assignments for ca. 70% of the H1' to H8/H6 connectivities. The ^{1}H-^{15}N long-range HSQC (Sklenář et al., 1994) can also in principle provide connectivities between base and H1' protons via nitrogen nuclei not directly bound to protons, but in practice on the relatively large ATP-binding aptamer correlations for only a few nucleotides were observed due to the very long transfer time needed. The major drawback of all of the HCN and ^{1}H-^{15}N long-range HSQC experiments is the high degree of overlap in the nitrogen dimension. This problem was resolved by the use of base-type selectively labeled RNA samples, as discussed below.

The assignment of the ribose spin systems for unlabeled RNA via 2D COSY and TOCSY spectra is limited by the narrow chemical shift range of the 2', 3', 4' and 5' protons

and the small (<3 Hz) H1'-H2' coupling constants for C3'-endo sugar puckers. With labeled RNA a strategy similar to the assignment of protein side chains can be applied, as described by Nikonowicz and Pardi (1993). A combination of 3D HCCH-TOCSY (Clore et al., 1990) and HCCH-COSY (Bax et al., 1990) experiments provides through-bond connectivities for the ribose protons and increases the resolution by exploiting the different carbon chemical shifts. HCCH experiments obtained on the fully labeled ATP binder allowed the assignment of many of the H1' and H4' ribose resonances. Assignment of the H2' and H3' resonances was limited by the severe overlap of the C2' and C3' resonances in the uniformly labeled sample, leading to many ambiguities for those protons at this point in the assignment procedure.

In principle, the best method to correlate the nucleotide spin systems is via the nucleic acid backbone. Unfortunately, these experiments do not in general give usable results with large RNAs due to the rapid relaxation of the involved nuclei and poor chemical shift dispersion of the phosphorus resonances. For the ATP-binding aptamer only the 2D versions of the HCP experiment (Marino et al., 1994b) were sensitive enough to give observable cross peaks, but the spectral overlap in the phosphorus dimension allowed only a few clear assignments to be made. The experiments correlating the sugar protons via combinations of PC and CCH transfers (Hare et al., 1983; Heus et al., 1994; Marino et al., 1995) suffered from low sensitivity, and gave fewer usable correlations than the 2D HCP. Overall, this class of experiments did not lead to any assignments beyond those which were easily obtainable from standard methods.

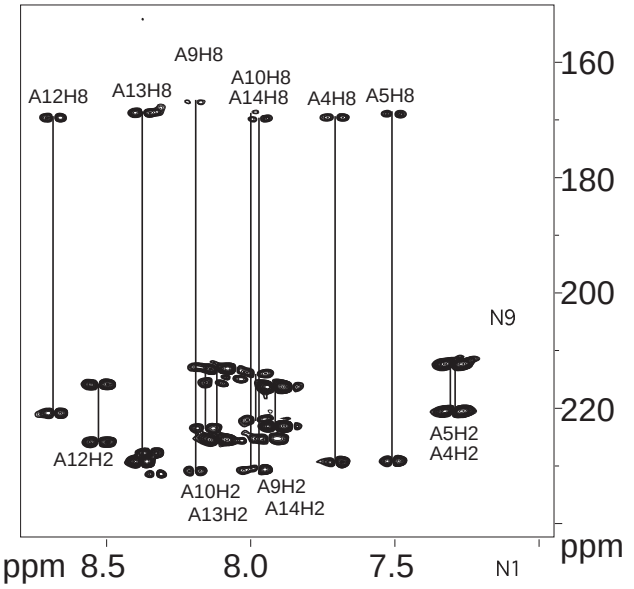

Fig. 8. ^{1}H-^{15}N long-range HSQC spectrum of an A-labeled RNA ATP binder in D_2O at 293 K. Correlations are observed for all seven adenine nucleotides in the aptamer. The lines connect corresponding N1/N3 and N9/N7 pairs correlated to the same proton (H2 and H8, respectively). The spectrum was acquired on a sample containing 0.9 mM of 1:1 RNA:AMP complex with 512 points in both dimensions using 256 scans per t_1 increment. The processed data matrix was 2048 × 2048 points and was apodized with a 60° and 75° shifted squared sine bell in t_2 and t_1 prior to transformation.

Base-type specifically labeled RNA in D_2O: Increased resolution provides additional assignments

NMR samples of the ATP-binding RNA aptamer containing labels only on G, A, or C/U nucleotides were essential for completing the assignments and identifying intra- and intermolecular NOEs. The major advantage of these samples is the greatly reduced signal overlap in filtered spectra. All of the above-described heteronuclear methods were applied to the partially labeled molecules and in general gave spectra which were better resolved and had fewer ambiguities. The gain in resolution for the base-type specifically labeled aptamer–AMP complexes can be visualized by a comparison of the HSQC of an A-labeled sample (Fig. 6) with the corresponding spectrum for the fully labeled sample (Fig. 5). In the spectrum of the A-labeled RNA, most of the cross peaks for the seven adenines in the sequence are resolved. The same is true for the 2D HCNCH experiment of a G-labeled sample shown in Fig. 7 – eight out of the 12 resonances present in the spectrum are completely resolved. The signals for G11 and G26 are missing due to the selective pulses that do not excite the strongly shifted C1'/H1' resonances of these residues. The reduced number of resonances also allowed the complete assignment of all base nitrogens, from a long-range ^{1}H-^{15}N HSQC experiment (Fig. 8).

The base-type specifically labeled ATP-binding aptamer samples were also useful for obtaining additional NOE restraints for structure calculations via filtered NOESY experiments, such as ^{13}C-filtered/selected 2D NOESY experiments (Otting and Wüthrich, 1990) (Fig. 9), in the same manner as applied for the study of protein–nucleic acid complexes. These experiments essentially sort the NOEs into three categories, i.e. NOEs between the labeled nucleotides, NOEs between the unlabeled nucleotides, and NOEs between labeled and unlabeled nucleotides. A series of these experiments acquired on the A, G, and C/U base-type specifically labeled samples of the aptamer complex allowed the unambiguous assignment of a large number of NOEs and the resolution of most of the remaining assignment ambiguities.

The only major assignment problem that could not be unambiguously resolved using these techniques was the identification of G11 and G30. These two nucleotides in the core of the internal loop and in close proximity to the ligand have very unusual NOE patterns with breaks in the sequential NOE connectivities and NOEs to a number of nonsequential nucleotides. None of the methods described above were able to clearly identify these two crucial spin systems.

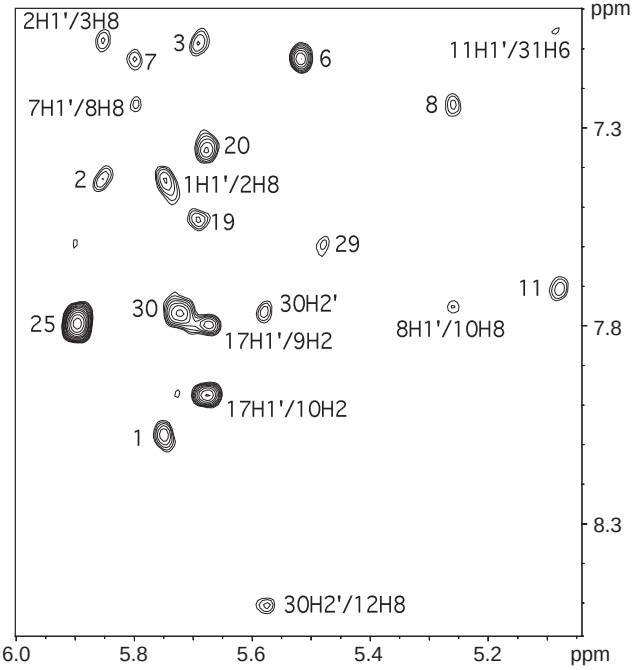

Fig. 9. H1' to base proton region of a 2D NOESY of a G-labeled RNA aptamer with ^{13}C selection in F2. Protons along the F2 axis are bound to carbon 13, whereas all protons can be detected along F1. Intranucleotide cross peaks are labeled by nucleotide number, and internucleotide NOEs are labeled by proton type and nucleotide. The spectrum was measured at 293 K with a mixing time of 200 ms on a sample containing 1.0 mM of 1:1 RNA:AMP complex. A standard X-filter was applied prior to the detection. In t_2 and t_1, 1024 and 256 complex points were acquired, respectively, with 128 scans per t_1 increment and States-TPPI phase cycling. The final data matrix was 2048×2048 points and was processed with a Gaussian filter function (LB −18, GB 0.08 in F2 and 0.14 in F1).

Fully and base-type specifically labeled $^{13}C,^{15}N$-labeled RNA in H_2O: Assignment of exchangeable protons

The exchangeable imino and amino protons are often located in the core of a folded nucleic acid, and thus can provide crucial NOE information. However, for the ATP-binding RNA aptamer the imino assignments for the residues in the internal loop region could not be obtained from the NOESY spectra alone, due to the unknown fold and unusual NOE patterns. The imino and amino resonances were first identified as to base type from ^{15}N-^{1}H HSQC or HMQC spectra acquired on a uniformly labeled sample in H_2O, using $1\bar{1}$-echo (Sklenář and Bax, 1987) or WATERGATE (Piotto et al., 1992; Sklenář et al., 1993c) sequences for suppression of the solvent signal. This allowed the assignment of the U16 imino (based on the fact that it is the only U in the internal loop and the unambiguous assignment of the stem iminos), but the assignment of the internal loop G-iminos was not possible based on the standard procedures since it could not be assumed that imino–imino NOEs were sequential. The HCCNH-TOCSY experiment (Sklenář et al., 1996), which gives direct correlations with the (already assigned) non-exchangeable base protons, was essential for the assignment of the imino resonances. Application of this experiment to a G-labeled sample is shown in Fig. 10. Similar techniques can be exploited to obtain direct correlations for aminos (Simorre et al., 1995,1996a,b; Fiala et al., 1996).

The presence of only certain types of labeled functional groups, like ^{15}N amino groups in the adenine- or cytosine/uridine-labeled RNA, allowed the straightforward identification of these protons and nitrogens (Fig. 11). In addition, filtered NOE experiments provided additional restraints for the structure calculation.

RNAs with single base mutations: Resolution of ambiguities

During the assignment process, ATP aptamers with single and multiple base substitutions were also studied to address specific assignment ambiguities as well as questions on hydrogen bond and base pairing interactions. Aptamers with base substitutions at nonconserved nucleotides (i.e. A9U, C15U, C18U/G29A) bound AMP with about the same affinity as wild-type and gave comparable spectra. Aptamers with base substitutions at conserved nucleotides generally bound AMP with lower affinity or not at all, but several of these aptamers (G7A, G8A, G17A) still bound AMP with high enough affinity to give usable spectra. The spectra were analyzed for changes in chemical shifts and NOE patterns. The mutant aptamers were used in an iterative process during the assignment procedure; based on a tentative assignment a mutant was designed to check if the spectra changed in the predicted way.

For the ATP-binding aptamer, the base-substituted aptamers were essential for resolving the previously mentioned problem of unambiguously identifying G11 and G30. For example, mutations in the vicinity of G30 (C18U/G29A mutant) shifted only signals belonging to one of the two guanine spin systems in question. On the other hand, a change of G7 (G7A mutant), which seemed to be base-paired to either G30 or G11, induced changes in the other guanine spin system (Fig. 12). This indirect evidence, together with trial structure calculations, provided the assignment for G30 and G11. These nucleotides have some very unusual and unpredicted NOE connectivities, including NOEs between G11 and C31 which showed the cross-peak pattern typically observed for sequential nucleotides, breaks in the NOE connectivities between A10 and G11 as well as G30 and G31, and NOEs between A12 and both G11 and G30.

In order to obtain additional evidence for the quite unexpected assignments of G11 and G30 (the assignment is reversed from what would be expected based purely on NOE patterns), we also prepared a deoxy G11 mutant of the aptamer. It was known from molecular biological studies that G11 deoxy still binds AMP, whereas the deoxy G30 mutant completely destroys any binding (Dieckmann et al., 1996). In addition, we observed a

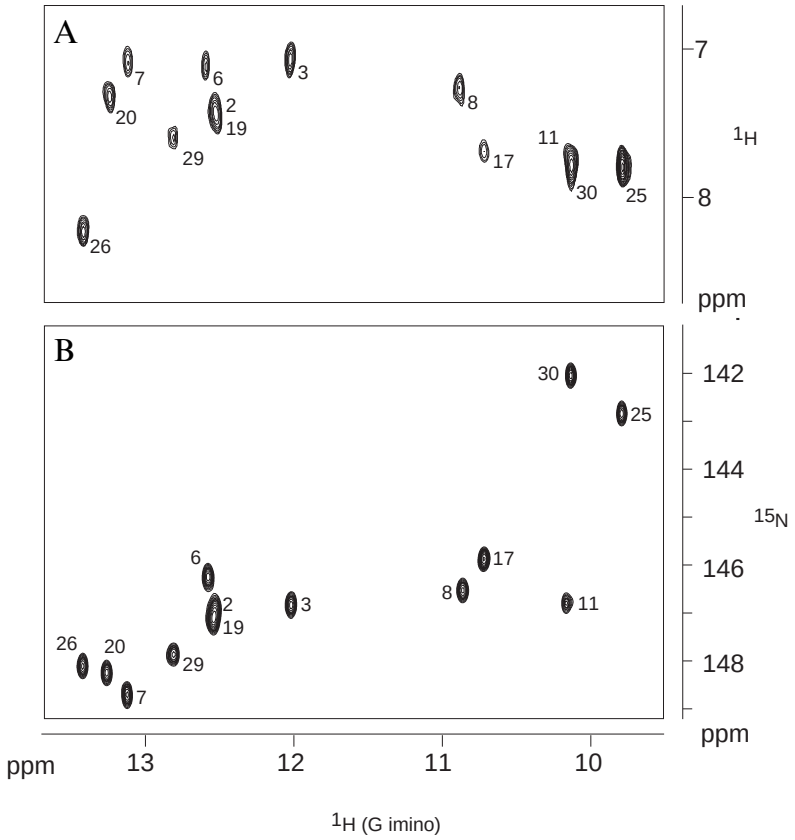

Fig. 10. (A) Two-dimensional HCCNH-TOCSY spectrum of a G-labeled RNA aptamer in complex with unlabeled AMP at 293 K (1.0 mM of 1:1 RNA:AMP complex), showing the cross peaks between the guanine imino protons and GH8 resonances. The spectrum was acquired with 48 $\times$2048 points in F1 and F2, respectively, and the DIPSI-2 mixing times were $\tau_1 = 77.4$ ms and $\tau_2 = 58$ ms. The size of the processed data matrix was 2048$\times$512 points. (B) Corresponding region of a ^{1}H-^{15}N HMQC with 1$\bar{1}$-echo water suppression measured on the same sample and conditions as in (A). In t_2 and t_1, 1024 and 64 complex points were acquired, respectively, with 128 scans per t_1 increment using States-TPPI phase cycling. The final data matrix was 1024$\times$512 points and was processed with a Gaussian filter function (LB –25, GB 0.1) in F2 and a 90° shifted squared sine bell in F1.

2'OH resonance at 9.3 ppm, which could be assigned to one of the two guanines (the one identified as G30) based on its characteristic NOE pattern and the unusual chemical shift of the 2' proton. A complex of the G11 deoxy mutant with AMP still shows the 2'-hydroxy signal and thus proves that the guanine with the 2'OH has to be G30.

Labeled AMP and unlabeled RNA: Assignment of ligand signals and identification of NOEs

Complete assignments of the bound ligand molecule were obtained using unlabeled RNA in complex with labeled AMP. Filtered NMR experiments allowed the observation of signals from the bound ligand without interference from the RNA signals. Assignments of the

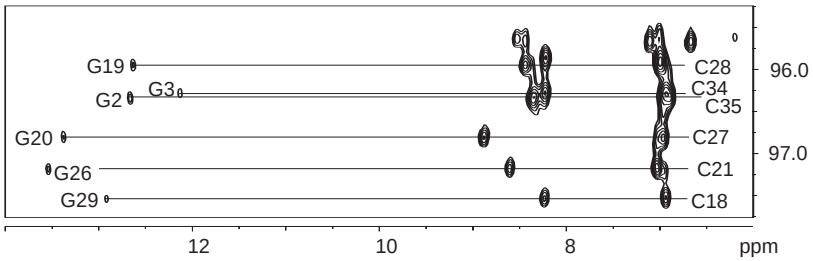

Fig. 11. Portion of a 2D ^{1}H-^{15}N HSQC-NOESY with 100 ms mixing time of a C- and U-labeled aptamer–AMP complex in H_2O; only the region with the C-amino cross peaks is shown. Nine out of the 10 C-aminos are visible; one pair lies outside the plotted region and does not show any NOE correlations. The spectrum was acquired with WATERGATE suppression of the H_2O resonance at 278 K on a sample containing 1.3 mM of RNA–AMP complex, with 1024$\times$64 complex points in F2 and F1, respectively, using 128 scans per t_1 increment. The processed data matrix was 1024$\times$1024 points and was apodized with a 60° and 90° shifted squared sine bell in t_2 and t_1 prior to transformation. NOE cross peaks between the C-aminos and G-iminos in the stem base pairs are labeled.

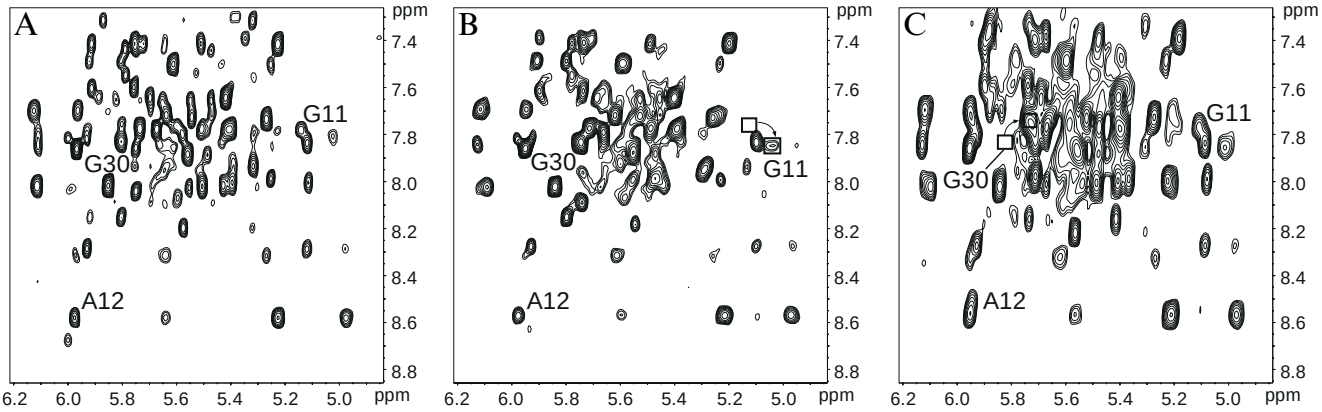

Fig. 12. H1' to base regions of 2D NOESY spectra of the wild-type aptamer (A) and mutant aptamers G7A (B) and C18UG29A (C) in complex with AMP. The spectra were acquired at 283 K on samples containing 1.4 mM (A), 0.7 mM (B), and 0.8 mM (C) of RNA–AMP complex. All acquisition parameters were kept identical, except the number of scans, which was doubled for the mutants. The spectra show the same overall distribution of signals. A good indicator for the proper fold of the complex is A12, which is located in the core of the folded molecule and interacting with the ligand. The position of its H1' and H8 as well as the pattern of NOE cross peaks observed for the H8 are basically identical in all three spectra, indicating the same fold. Some of the cross peaks that are shifted compared to their position in the wild-type spectrum are marked by boxes. All spectra were acquired in D_2O with low-power saturation of the residual HDO resonance. 1024 and 64 complex points in F2 and F1, respectively, with 64 (128 for the mutants) scans per t_1 increment were acquired. States-TPPI phase cycling was applied in F1. The final data matrices were 2048×1024 points and were processed with a Gaussian filter function (LB –25, GB 0.1) in F2 and a 90° shifted squared sine bell in F1.

AMP resonances were made by comparison with ^{1}H-^{13}C and ^{1}H-^{15}N HSQC cross peaks of the unbound AMP in a sample containing a slight excess of AMP.

The identification of intermolecular NOEs was carried out in a similar manner to the well-established methodology developed for protein–ligand systems (Otting et al., 1990; Otting and Wüthrich, 1990). ^{13}C- or ^{15}N-filtered NOESY experiments allowed the selective observation of these NOEs. Due to the presence of only labeled AMP in these samples, 1D and 2D NMR techniques provided enough resolution to resolve all crucial cross peaks. For example, NOEs involving the AMP amino group were identified from a 1D ^{15}N-filtered NOESY. Carbon-filtered 2D NOESY experiments in H_2O using a water flip-back

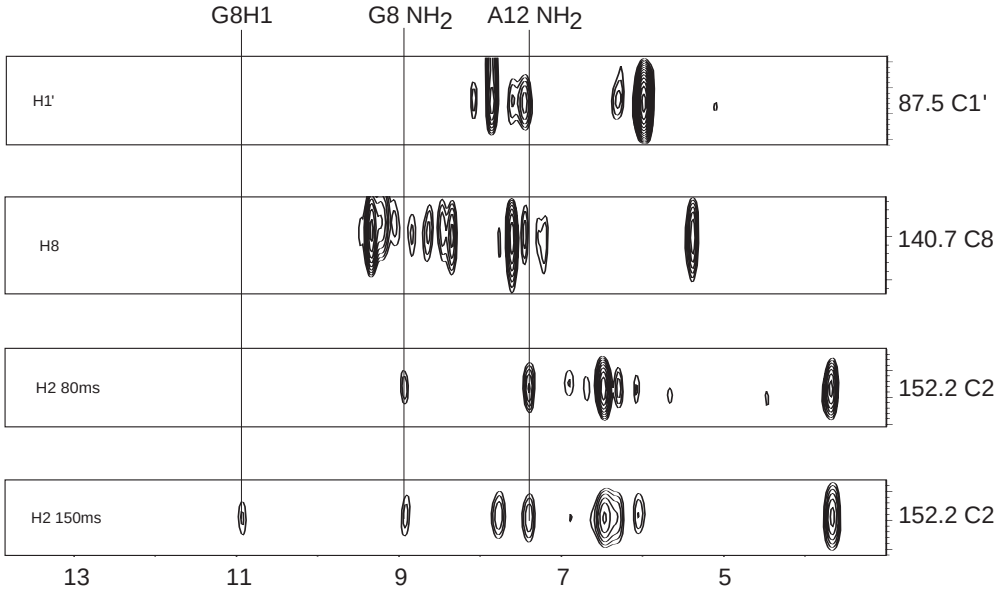

Fig. 13. Traces out of 2D ^{1}H-^{13}C HSQC-NOESY spectra in H_2O, measured on a sample containing unlabeled RNA and ^{15}N,^{13}C-labeled AMP. The traces are taken at the ^{13}C chemical shifts of C1', C8, and C2. The traces for H2/C2 (C and D) are from spectra with NOESY mixing times of 80 and 150 ms (C and D, respectively), illustrating that the NOE cross peak between G8 H1 and AMP H2 is due to spin diffusion, probably via the amino. Several crucial NOEs are labeled. A WATERGATE sequence in combination with a water flip-back pulse was applied for solvent suppression; 1024×128 complex points in F2 and F1 were acquired, respectively, using 128 scans per t_1 increment. The processed data matrix was 2048×1024 points and was apodized with a 60° and 90° shifted squared sine bell in t_2 and t_1 prior to transformation.

TABLE 2
^{1}H, ^{13}C, AND ^{15}N ASSIGNMENTS FOR THE CORE REGION OF THE ATP-BINDING RNA APTAMER (NUCLEOTIDES 6–18, 29–31, AND AMP) AT 283 K, pH 6.0 IN 100 mM NaCl

Residue	H8/6 (C8/6)	H2/5 (C2/5)	H1' (C1')	H2' (C2')	H3' (C3')	H4' (C4')	H5' (C5')	NH_2 (N)	NH (N)	N7	N9	N1	N3
G6	7.18 (131.7)	–	5.58 (89.8)	4.00 (73.1)		4.33 (79.2)			12.67 (146.0)	237.2	169.1	–	–
G7	7.18 (131.7)	–	5.88 (89.9)	4.41 (73.7)	4.59 (69.0)	4.37 (79.1)			13.30 (148.5)	232.8	169.1	–	–
G8	7.31 (137.3)	–	5.32 (91.6)	4.32 (73.0)	4.73 (68.9)	4.30 (79.7)		8.98/5.06 (75.1)	10.95 (146.3)	238.0	170.7	–	–
A9	8.19 (140.1)	7.85 (151.8)	5.51 (91.3)	4.69 (73.2)	4.44 (68.6)	4.17 (79.8)	4.05/4.16 (64.5)		–	230.2	168.4	212.7	223.3
A10	7.80 (140.1)	8.03 (153.2)	6.05 (86.4)	3.63 (74.8)		4.40 (80.8)			–	230.9	166.9	213.9	221.7
G11	7.78 (139.1)	–	5.14 (82.9)	4.34 (75.5)	4.54 (71.3)	1.67 (82.9)	3.06/3.60 (65.0)		10.38 (146.5)	233.5	164.0	–	–
A12	8.57 (139.1)	8.42 (155.2)	5.92 (87.6)	5.16 (71.3)	4.91 (77.0)	4.52 (83.9)		7.40/6.51 (84.6)	–	220.7	169.2	215.8	225.7
A13	8.28 (139.4)	7.70 (151.7)	5.88 (91.2)	5.05 (72.2)	4.56	4.41 (79.0)			–	229.0	168.4	213.0	225.4
A14	7.82 (137.2)	7.91 (152.6)	5.61 (89.5)	4.34 (72.7)	4.63 (68.7)	4.42 (79.0)			–	230.4	169.4	216.2	222.3
C15	7.07 (136.8)	5.44 (95.5)	5.25 (91.2)	4.18 (73.3)	4.14 (69.2)	4.27 (78.9)	4.36/4.02 (61.8)		–	–	–		
U16	7.50 (137.2)	5.62 (102.0)	5.54 (91.4)	4.48 (69.7)				–	10.21 (154.4)	–	–		–
G17	7.75 (135.8)	–	5.75 (90.3)	4.41					10.89 (145.7)	234.3	168.6	–	–
C18	7.93 (138.6)	5.32 (95.7)	6.28 (91.1)	4.63				8.27/7.00 (99.8)	–	–	–		
G29	7.65 (132.0)	–	5.55 (91.5)	4.38 (72.8)	4.74 (70.2)	4.33 (80.0)			12.87 (147.6)	233.5	168.5	–	–
G30	7.83 (138.5)	–	5.81 (88.1)	5.64 (67.5)	4.93 (72.7)	4.69 (83.6)			10.36 (141.8)	238.5	160.2	–	–
C31	7.11 (138.3)	5.30 (94.6)	5.12 (92.2)	4.27 (70.3)	3.79 (69.0)	4.36 (79.4)	4.10/4.44 (63.4)		–	–	–		
AMP	8.62 (140.7)	6.45 (152.2)	5.94 (87.5)	4.83 (79.4)	4.76 (73.8)	4.66 (86.6)	4.16/4.23 (68.3)	7.88/7.00 (83.1)	–	236.0	164.9	216.2	222.2

All chemical shifts (ppm) are referenced relative to the HDO signal at 4.89 ppm.

WATERGATE for the suppression of the solvent signal resolved three NOEs between the nonexchangeable protons of the AMP and exchangeable RNA protons (Fig. 13).

Identification of possible hydrogen bonds

The identification of H-bonds by NMR spectroscopy is problematic, as there are currently no generally accepted criteria for this purpose. However, during the course of the assignments and the structure calculation a lot of indirect evidence for H-bonds was gathered. The major sources of information are the observed NOE patterns, especially for the exchangeable NOEs, and the exchange behavior of the involved protons. The nitrogen chemical shifts give some additional evidence for the presence or absence of H-bonds. For example, the imino and amino nitrogen resonances of nucleotides involved in Watson–Crick base pairs are generally found at lower field than those originating from imino nitrogens of non-base-paired nucleotides. The imino nitrogens of the stem nucleotides of the ATP-binding aptamer are found at ~147 ppm (G) and ~162 ppm (U), whereas the imino nitrogen of U22 (which is not H-bonded in the UUCG loop) is found at 159.1 ppm. A similar chemical shift difference of 3–5 ppm is found for the amino group in bound and free AMP (not shown). Nitrogens which act as H-bond acceptors are shifted towards higher field. For example, the N7 of A12 (which is H-bonded to G30 2'OH) appears at 220.7 ppm, compared to an average chemical shift for AN7 of ~230 ppm (Fig. 8).

For the ATP-binding aptamer the existence of an H-bond in the internal loop region was assumed only if all of the following criteria were fulfilled: (i) structure calculations without using the H-bonds as input restraints resulted in local geometries consistent with the existence of an H-bond with respect to the angle and distance of the involved atoms; (ii) the involved exchangeable protons

had line widths comparable to those of the base pairs within the stem region, which are clearly involved in stable H-bonds; and (iii) the chemical shifts of all involved nuclei and the chemical shift differences between bound and unbound form are consistent with the formation of an H-bond.

Conclusions

Nucleic acids, especially RNA, present problems in NMR assignment that are significantly different from those of proteins. The development of NMR methods exploiting ^{13}C,^{15}N labels in RNA has helped substantially in expanding the possibilities for assignment. In spite of the advantages of spectra acquired on uniformly ^{13}C,^{15}N-labeled RNA, they still do not provide a reliable pathway for obtaining direct, through-bond sequential assignments in larger RNA oligonucleotides (more than 30 nucleotides). We have developed and applied a variety of heteronuclear experiments to the study of the ATP-binding aptamer. Complete sequential proton (base, H1', H2') assignments as well as the majority of other ^{1}H and ^{15}N and ^{13}C assignments for the ATP-binding aptamer (Table 2) were only obtained by a combination of heteronuclear NMR techniques applied to samples which had been selectively labeled at all G, A, or C/U nucleotides and comparison of unlabeled wild-type aptamer spectra to spectra obtained on samples with specific base substitutions. The use of base-type selectively labeled samples also greatly increased the number of NOEs that could reliably be used in the structure calculations.

Of crucial importance for the structure determination of the ATP-binding RNA aptamer was the unambiguous assignment of as many exchangeable proton resonances as possible. These assignments are critical to obtaining the correct fold and hydrogen bonding interactions in RNA. As with the sequential assignment of nonexchangeable resonances, the assignment of exchangeable resonances using proton-only methods relies on the assumption of a helical structure. For the ATP-binding aptamer, assignments of the loop iminos could only be obtained by application of the HCCNH experiment (Fiala et al., 1996; Sklenář et al., 1996), which was developed specifically for the purpose of assigning imino resonances in nonhelical structures.

The assignment strategy discussed here points the way towards future studies of even larger RNAs. In addition to the selective base-type labels used here, studies on larger RNAs may also require selective use of deuterium-labeled nucleotides (Tolbert and Williamson, 1996).

Acknowledgements

This work was supported by grants from NSF (MCB-9506913) and NIH (GM 39558) to J.F. and an HFSPO long-term postdoctoral fellowship to T.D. We also acknowledge the Los Alamos Stable Isotope facility for providing labeled cells.

References

Allain, F. and Varani, G. (1995) *J. Mol. Biol.*, **250**, 333–353.

Batey, R.T., Inada, M., Kujawinski, E., Puglisi, J.D. and Williamson, J.R. (1992) *Nucleic Acids Res.*, **20**, 4515–4523.

Battiste, J.L., Tan, R., Frankel, A.D. and Williamson, J.R. (1995) *J. Biomol. NMR*, **6**, 375–389.

Bax, A., Clore, G.M., Driscoll, P.C., Gronenborn, A.M., Ikura, M. and Kay, L.E. (1990) *J. Magn. Reson.*, **87**, 620–627.

Cavanagh, J., Fairbrother, W.J., Palmer, A.G.I. and Skelton, N.J. (1996) *Protein NMR Spectroscopy: Principles and Practice*, Academic Press, San Diego, CA, U.S.A.

Cheong, C., Varani, G. and Tinoco Jr., I. (1990) *Nature*, **346**, 680–682.

Clore, G.M., Bax, A., Driscoll, P.C., Wingfield, P.T. and Gronenborn, A.M. (1990) *Biochemistry*, **29**, 8172–8184.

Clore, G.M. and Gronenborn, A.M. (1993) *NMR of Proteins*, CRC Press, Boca Raton, FL, U.S.A.

Dieckmann, T. and Feigon, J. (1994) *Curr. Opin. Struct. Biol.*, **4**, 745–749.

Dieckmann, T., Suzuki, E., Nakamura, G.K. and Feigon, J. (1996) *RNA*, **2**, 628–640.

Ellington, A.D. and Szostak, J.W. (1990) *Nature*, **346**, 818–822.

Farmer II, B.T., Müller, L., Nikonowicz, E.P. and Pardi, A. (1993) *J. Am. Chem. Soc.*, **115**, 11040–11041.

Feigon, J., Leupin, W., Denny, W.A. and Kearns, D.R. (1983) *Biochemistry*, **22**, 5943–5951.

Feigon, J., Sklenář, V., Wang, E., Gilbert, D.E., Macaya, R.F. and Schultze, P. (1992) *Methods Enzymol.*, **211**, 235–254.

Feigon, J., Dieckmann, T. and Smith, F.W. (1996) *Chem. Biol.*, **3**, 611–617.

Fiala, R., Jiang, F. and Patel, D.J. (1996) *J. Am. Chem. Soc.*, **118**, 689–690.

Hare, D.R., Wemmer, D.E., Chou, S.-H., Drobny, G.P. and Reid, B.R. (1983) *J. Mol. Biol.*, **171**, 319–336.

Heus, H.A., Wijmenga, S.S., Van de Ven, F.J.M. and Hilbers, C.W. (1994) *J. Am. Chem. Soc.*, **116**, 4983–4984.

Jiang, F., Kumar, R.A., Jones, R.A. and Patel, D.J. (1996) *Nature*, **382**, 183–186.

Legault, P., Farmer II, B.T., Müller, L. and Pardi, A. (1994) *J. Am. Chem. Soc.*, **116**, 2203–2204.

Marino, J.P., Prestegard, J.H. and Crothers, D.M. (1994a) *J. Am. Chem. Soc.*, **116**, 2205–2206.

Marino, J.P., Schwalbe, H., Anklin, C., Bermel, W., Crothers, D.M. and Griesinger, C. (1994b) *J. Am. Chem. Soc.*, **116**, 6472–6473.

Marino, J.P., Schwalbe, H., Anklin, C., Bermel, W., Crothers, D.M. and Griesinger, C. (1995) *J. Biomol. NMR*, **5**, 87–92.

Marion, D., Kay, L.E., Sparks, S.W., Torchia, D.A. and Bax, A. (1989) *J. Am. Chem. Soc.*, **111**, 1515–1517.

Michnicka, M.J., Harper, J.W. and King, G.C. (1993) *Biochemistry*, **32**, 395–400.

Milligan, J.F., Groebe, D.R., Witherell, G.W. and Uhlenbeck, O.C. (1987) *Nucleic Acids Res.*, **15**, 8783–8798.

Moore, P.B. (1993) *Curr. Opin. Struct. Biol.*, **3**, 340–344.

Müller, L., Nikonowicz, E.P., Farmer II, B.T. and Pardi, A. (1994) *J. Biomol. NMR*, **4**, 129–133.

Nikonowicz, E.P., Sirr, A., Legault, P., Jucker, F.M., Baer, L.M. and Pardi, A. (1992) *Nucleic Acids Res.*, **20**, 4507–4513.

Nikonowicz, E.P. and Pardi, A. (1993) *J. Mol. Biol.*, **232**, 1141–1156.

Otting, G., Qian, Y.Q., Billeter, M., Müller, M., Affolter, M., Gehring, W.J. and Wüthrich, K. (1990) *EMBO J.*, **9**, 3085–3092.

Otting, G. and Wüthrich, K. (1990) *Q. Rev. Biophys.*, **23**, 39–96.

Pardi, A. (1995) *Methods Enzymol.*, **261**, 350–380.

Peterson, R.D., Bartel, D.P., Szostak, J.W., Horvath, S.J. and Feigon, J. (1994) *Biochemistry*, **33**, 5357–5366.

Piantini, U., Sørensen, O.W. and Ernst, R.R. (1982) *J. Am. Chem. Soc.*, **104**, 6800–6801.

Piotto, M., Saudek, V. and Sklenář, V. (1992) *J. Biomol. NMR*, **2**, 661–665.

Santoro, J. and King, G. (1992) *J. Magn. Reson.*, **97**, 202–207.

Sassanfar, M. and Szostak, J.W. (1993) *Nature*, **364**, 550–553.

Scheek, R.M., Russo, N., Boelens, R. and Kaptein, R. (1983) *J. Am. Chem. Soc.*, **105**, 2914–2916.

Simorre, J.-P., Zimmermann, G.R., Pardi, A., Farmer II, B.T. and Müller, L. (1995) *J. Biomol. NMR*, **4**, 427–432.

Simorre, J.-P., Zimmermann, G.R., Müller, L. and Pardi, A. (1996a) *J. Biomol. NMR*, **7**, 153–156.

Simorre, J.-P., Zimmermann, G.R., Müller, L. and Pardi, A. (1996b) *J. Am. Chem. Soc.*, **118**, 5316–5317.

Sklenář, V. and Bax, A. (1987) *J. Magn. Reson.*, **74**, 469–479.

Sklenář, V., Peterson, R.D., Rejante, M.R. and Feigon, J. (1993a) *J. Biomol. NMR*, **3**, 721–727.

Sklenář, V., Peterson, R.D., Rejante, M.R., Wang, E. and Feigon, J. (1993b) *J. Am. Chem. Soc.*, **115**, 12181–12182.

Sklenář, V., Piotto, M., Leppik, R. and Saudek, V. (1993c) *J. Magn. Reson.*, **A102**, 241–245.

Sklenář, V., Peterson, R.D., Rejante, M.R. and Feigon, J. (1994) *J. Biomol. NMR*, **4**, 117–122.

Sklenář, V., Dieckmann, T., Butcher, S.E. and Feigon, J. (1996) *J. Biomol. NMR*, **7**, 83–87.

Tate, S.-I., Ono, A. and Kainosho, M. (1994) *J. Am. Chem. Soc.*, **116**, 5977–5978.

Tolbert, T.J. and Williamson, J.R. (1996) *J. Am. Chem. Soc.*, **118**, 7929–7940.

Tuerk, C. and Gold, L. (1990) *Science*, **249**, 505–510.

Varani, G. and Tinoco, I. (1991) *Q. Rev. Biophys.*, **24**, 479–532.

Varani, G., Aboul-ela, F. and Allain, F.H.T. (1996) *Prog. NMR Spectrosc.*, **29**, 51–127.

Vuister, G.W. and Bax, A. (1992) *J. Magn. Reson.*, **98**, 428–435.

Wüthrich, K. (1986) *NMR of Proteins and Nucleic Acids*, Wiley, New York, NY, U.S.A.

Zuiderweg, E.R.P., McIntosh, L.P., Dahlquist, F.W. and Fesik, S.W. (1990) *J. Magn. Reson.*, **86**, 210–216.

Zuiderweg, E.R.P., Petros, A.M., Fesik, S.W. and Olejniczak, E.T. (1991) *J. Am. Chem. Soc.*, **113**, 370–372.